The Virgo interferometric gravitational antenna

F. Acernese, P. Amico, M. Al-Shourbagy, S. Aoudia, S. Avino, D. Babusci, G. Ballardin, R. Barillé, F. Barone, L. Barsotti, et al.

The Virgo interferometric gravitational antenna

F. Acernese[‖], P. Amico[x], M. Al-Shourbagy[xi], S. Aoudia[**], S. Avino[‖], D. Babusci[§], G. Ballardin[†], R. Barillé[†], F. Barone[‖], L. Barsotti[xi], M. Barsuglia[††], F. Beauville[*], M. A. Bizouard[††], C. Boccara[‡‡], F. Bondu[**], L. Bosi[x], C. Bradaschia[xi], S. Braccini[xi], A. Brillet[**], V. Brisson[††], L. Brocco[xii], D. Buskulic[*], E. Calloni[‖], E. Campagna[‡], F. Cavalier[††], R. Cavalieri[†], G. Cella[xi], E. Chassande-Mottin[**], C. Corda[xi], A.-C. Clapson[††], F. Cleva[**], J.-P. Coulon[**], E. Cuoco[†], V. Dattilo[†], M. Davier[††], R. De Rosa[‖], L. Di Fiore[‖], A. Di Virgilio[xi], B. Dujardin[**], A. Eleuteri[‖], D. Enard[†], I. Ferrante[xi], F. Fidecaro[xi], I. Fiori[xi], R. Flaminio[*], J.-D. Fournier[**], S. Frasca[xii], F. Frasconi[†], A. Freise[†], L. Gammaitoni[x], A. Gennai[xi], A. Giazotto[xi], G. Giordano[§], L. Giordano[‖], R. Gouaty[*], D. Grosjean[*], G. Guidi[‡], S. Hebri[†], H. Heitmann[**], P. Hello[††], L. Holloway[†], S. Kreckelbergh[††], P. La Penna[†], V. Loriette[‡‡], M. Loupias[†], G. Losurdo[‡], J.-M. Mackowski[¶], E. Majorana[xii], C. N. Man[**], M. Mantovani[xi], F. Marchesoni[x], F. Marion[*], J. Marque[†], F. Martelli[‡], A. Masserot[*], M. Mazzoni[‡], L. Milano[‖], C. Moins[†], J. Moreau[‡‡], N. Morgado[¶], B. Mours[*], A. Pai[xii], C. Palomba[xii], F. Paoletti[†], S. Pardi[‖], A. Pasqualetti[†], R. Passaquieti[xi], D. Passuello[xi], B. Perniola[‡], F. Piergiovanni[‡] L. Pinard[¶], R. Poggiani[xi], M. Punturo[x], P. Puppo[xii], K. Qipiani[‖], P. Rapagnani[xii], V. Reita[‡‡], A. Remillieux[¶], F. Ricci[xii], I. Ricciardi[‖], P. Ruggi[†], G. Russo[‖], S. Solimeno[‖], A. Spallicci[**], R. Stanga[‡], R. Taddei[†], D. Tombolato[*], M. Tonelli[xi], A. Toncelli[xi], E. Tournefier[*], F. Travasso[x], G. Vajente[xi], D. Verkindt[*], F. Vetrano[‡], A. Viceré[‡], J.-Y. Vinet[**], H. Vocca[x], M. Yvert[*] and Z. Zhang[†]

[*] Laboratoire d'Annecy-le-Vieux de Physique des Particules, Annecy-le-Vieux, France;

[†] European Gravitational Observatory (EGO), Cascina (Pi), Italia;

[‡] INFN, Sezione di Firenze/Urbino, Sesto Fiorentino, and/or Università di Firenze, and/or Università di Urbino, Italia;

[§] INFN, Laboratori Nazionali di Frascati, Frascati (Rm), Italia;

[¶] LMA, Villeurbanne, Lyon, France;

[‖] INFN, sezione di Napoli and/or Università di Napoli "Federico II" Complesso Universitario di Monte S. Angelo, and/or Università di Salerno, Fisciano (Sa), Italia;

[**] Departement Artemis – Observatoire de la Côte d'Azur, BP 42209 06304

Nice, Cedex 4, France;
[††] Laboratoire de l'Accélérateur Linéaire (LAL), IN2P3/CNRS-Univ. de Paris-Sud, Orsay, France;
[††] ESPCI, Paris, France;
[x] INFN, Sezione di Perugia and/or Università di Perugia, Perugia, Italia;
[xi] INFN, Sezione di Pisa and/or Università di Pisa, Pisa, Italia;
[xii] INFN, Sezione di Roma and/or Università "La Sapienza", Roma, Italia.

E-mail: Corresponding author: P. La Penna <paolo.lapenna@ego-gw.it>

Abstract. The interferometric gravitational wave detectors represent the ultimate evolution of the classical Michelson interferometer. In order to measure the signal produced by the passage of a gravitational wave, they aim to reach unprecedent sensitivities in measuring the relative displacements of the mirrors. One of them, the 3-km-long Virgo gravitational wave antenna, which will be particularly sensitive in the low frequency range (10-100 Hz), is presently in its commissioning phase. In this paper the various techniques developed in order to reach its target extreme performance are outlined.

Submitted to: Class. Quantum Grav.

PACS numbers: 04.80.Nn, 95.55.Ym

1. Introduction

The present ground-based interferometrical gravitational wave detectors Virgo [2], LIGO [3], TAMA300 [4], GEO600 [5]) aim to reach a spectral strain sensitivity of h about $10^{-23}/\sqrt{Hz} - 10^{-22}/\sqrt{Hz}$ in a frequency range around 100 Hz. This means, in terms of relative displacements of the test masses, to measure length varitions of less than $10^{-19} m/\sqrt{Hz}$ (see figure 1). In order to reach this extreme sensitivity, special optical configurations have been developed.

The passage of a gravitational wave can be detected in the output interferometric signal as a relative displacement of a set of quasi-free falling masses (suspended mirrors). Virgo, mainly consisting of a 3-km-long Michelson interferometer, with Fabry-Perot cavities in the arms and power recycling, shares with other experiments, such as LIGO [3], TAMA [4] and GEO [5], substantially the same optical detection principle, and it aims to detect gravitational waves emitted by astrophysical sources [2] in a frequency range between a few Hz and a few kHz. In particular, Virgo, thanks to its peculiar attenuating system providing the highest passive isolation performance, will be more sensitive than the other detectors at low frequency (10-100 Hz range), aiming at a displacement sensitivity of $10^{-17} m/\sqrt{Hz}$ at 10 Hz and at the level $10^{-19} m/\sqrt{Hz}$ at about 100 Hz. In terms of fringe sensitivity, the progress with respect to the Michelson and Morley experiment would be from their 1/100 [1] to the present $1/10^{12}$ of the fringe (but the frequency reange at which the measurement is performed is different).

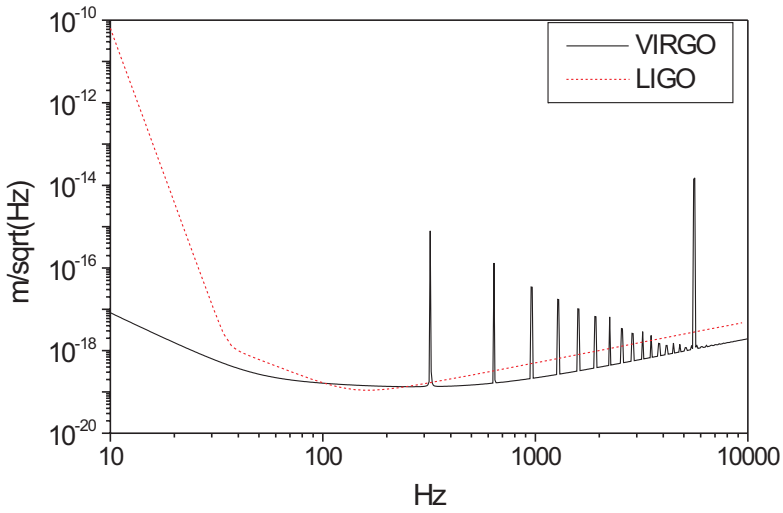

Figure 1. Comparison of the design displacement sensitivity of the two interferometers Virgo and LIGO, expressed in $m/\sqrt{Hz}$, as a function of the frequency.

2. Basic principles of operation of an interferometric antenna

The first idea of the interferometric detection of gravitational waves remounts up to the 60's[6]. The passage of a gravitational wave, coming from a direction perpendicular to the line connecting two mirrors, suspended as quasi-free test masses at a certain distance L one from the other, will be seen by a laser light beam travelling along this line as a displacement of the same test masses. The result will be a change in the interference condition between the beams coming from the two opposite directions. Since the action of the gravitational wave on a length L is essentially described by its adimensional strain $h = \Delta L/L$, the quantity ΔL to be measured is enhanced if the length L is larger. Given the expected values for an adimensional strain of astrophysical source (about $10^{-23}/\sqrt{Hz} - 10^{-22}/\sqrt{Hz}$ in the 10-100 Hz frequency range), the ΔL to be measured is extremely small. For this reason the ground based gravitational wave interferometers are as long as possible, of the order of several km (Virgo is 3 km long, LIGO is 4 km long).

2.1. Optical cavities

In order to increase the optical path, the first possibility would be to use delay lines: the light could be made travel many times inside two mirrors spaced several km apart. This device is too difficult to control, thus the use of optical cavities (Fabry-Perot) has been preferred. In a Fabry-Perot cavity having finesse F the dephasing of the reflected light is enhanced by a factor $2/\pi \times F$. Therefore, with a finesse $F = 50$, a cavity 3-km -long can be seen as optically equivalent to an about 120-km -long one.

2.2. Michelson configuration

In principle a single cavity could be used. However, the signal coming from a single cavity would be dominated by the laser frequency noise $\Delta\nu$ (typically of the order of $10^4 Hz/(f\sqrt{Hz})$. For a cavity having length L of the order of 1 km, and a laser frequency $\nu = 2.8 \times 10^{14}$, the equivalent displacement noise would be $\Delta L = \Delta\nu/\nu \times L \cong 3 \times 10^{-10} Hz/\sqrt{Hz}$ at 100 Hz. In order to overcome this limit the interferometer configuration is used: in an ideal Michelson, having no arms asymmetry, there is no frequency noise injection in the interference between the beams coming from the two arms. This is the reason because all the gravitational antennas have the Michelson interferometer configuration. In a gravitational wave interferometric antenna high-quality optics are suspended to act as quasi-free test masses at the end of the Michelson interferometer arms, the arms being, in Virgo, LIGO and TAMA, optical cavities.

2.3. Dark fringe

Using laser beams, the first fundamental noise source is the shot noise connected to the corpuscular nature of the light. In order to improve the shot noise signal-to-noise ratio, it can be shown that the shot noise signal to noise ration is maximized if the interferometer is kept on the dark fringe, that is the two beams coming from the two arms are made destructively interfering. All the light is therefore reflected back towards the laser source. In this way, the whole interferometer behaves like a mirror, reflecting back all the incoming light. Since the shot noise signal-to-noise ratio improves with the square root of the power, it is convenient to increase as much as possible the light stored inside the interferometer.

2.4. Power recycling

Once the limit in the increase of the incoming laser power is reached, a further improvement can be obtained by reflecting again, towards the interferometer, the light coming back to the laser. For this reason, between the laser and the interferometer beam splitter, another mirror, called the recycling mirror, is placed, which, together with the interferometer itself, forms a further optical cavity in which the light is stored. The light power inside the recycling cavity, i.e. the light impinging onto the interferometer beam splitter, is enhanced by a "recycling" factor.

2.5. Heterodyne detection

A further limit to the sensitivity are the power fluctuations of the laser light. The presently available noise source are not shot noise dominated in the frequency of interest for gravitational wave detection (10 Hz-10 kHz). One trick to overcome the power fluctuation problem is to shift the detection frequency in a frequency range where the laser beam is shot noise dominated. For this reason the laser light is modulated in phase at a frequency of several MHz, where the laser is shot noise dominated, before entering the interferometer, and then demodulated by the same reference, in the standard Pound-Drever-Hall (PDH) scheme [7] [8]. At the dark fringe output of the interferometer the beating between the carrier and the

sidebands is detected (heterodyne detection), when the destructive interference condition is modified by the passage of a gravitational wave. In order to have an available signal, the sidebands have to be partially transmitted to the dark port: this is obtained by introducing a slight asymmetry in the arms length, so that when the carrier is on the perfect destructive interference the sidebands are partially transmitted (Schnupp's technique [9]).
The arms asymmetry imposed by the Schnupp's technique, together with other arms asymmetries (like cavity finesse asymmetries), have as a consequence that part of the frequency noise of the laser is reintroduced in the interferometer. This imposes to stabilize the laser frequency, up to a level where its effect is lower than the shot noise (the frequency stabilization scheme adopted in Virgo will be described in 4.3.

2.6. Automatic alignment

In addition to the interferometer is longitudinal locking, an angular control system is needed to maintain the mirrors in an aligned position with respect to one another and the incoming beam. The alignment system is not referred to the ground, it rather keeps the interferometer automatically aligned on the incoming beam. Several techniques, known as wavefront sensing techniques [10] are used in the gravitational wave interferometers: they all take advantage, analogously to the Pound-Drever-Hall technique, of a high frequency (MHz) modulation-demodulation technique. The automatic alignment scheme designed for Virgo [12] uses the Anderson technique [11]. The modulation frequency is chosen so that the first order transverse modes (TEM_{01}) of the sidebands are resonant in the arm cavities. Once all the cavities of the interferometer are locked at their resonance, the transmitted light is detected by differential wave-front sensors, producing photo currents which are demodulated and then opportunely mixed to achieve signals proportional to the misalignments between the optical components. These signals are then filtered and sent by feedback to the mirrors at the level of the marionette with a control bandwidth of a few Hz, so that noise is not reintroduced in the detection band.

2.7. Locking

In order to attain the desired sensitivity, the interferometer has to be placed and kept in a specified working point, i.e. with the arms at the optical resonance of the cavities, the Michelson on the output dark fringe and the recycling cavity at its resonance. This means that the various lengths and positions of the mirrors have to be actively controlled, this operation being called longitudinal locking of the interferometer.

3. The Virgo interferometer

3.1. Virgo general layout

The optical layout of Virgo is shown in figure 2: a laser beam (20W @ 1064nm) is produced by a $Nd:YVO_4$ high power laser injection, locked to a 1W Nd:YAG master laser. The laser light

is modulated in phase at a frequency of 6.26 MHz before entering the vacuum system at the injection bench (IB), and is then pre-stabilized by the 144 m long input mode-cleaner (IMC), to a few tens of kHz using a standard Pound-Drever-Hall (PDH) scheme [7][8]. The low frequency pre-stabilization is performed by actively controlling the length of the IMC to lock the laser frequency to the length of a 30 cm monolithic triangular cavity (RFC) suspended in vacuum. A 10 W power beam emitted from the injection system enters into the interferometer (ITF) through the power-recycling mirror (PR). The beam is split at the level of the beam-splitter mirror (BS), and enters the two 3km long Fabry-Perot cavities (north cavity and west cavity).
Together with the PR mirror, the Michelson ITF forms a Febry-Perot cavity, the power recycling cavity, with an optical recycling gain of 50 when the ITF is at its working point. In this state, the expected power upon the BS is 500 W. The 3-km Fabry-Perot cavities have a finesse of 50 (optical gain about 32): the final power circulating inside the ITF is therefore estimated to be around 8 kW. With the ITF at the operating point, the gravitational wave signal is extracted on the dark port beam, which passes through the output mode-cleaner (OMC), to reach a set of 16 InGaAS photodiodes (B1), by which the dark port signal is reconstructed. Other signals are extracted from the ITF, essentially for control purposes: figure 2 shows the benches detecting the beams transmitted by the long Fabry-Perot cavities (NB and WB), the beam reflected by the ITF (DT), and the beam reflected by the second face of the BS (DB). In figure 3 the noise sources limiting the Virgo sensitivity are shown: the main limiting noise contributions will be seismic disturbances below 4 Hz, thermal noise up to 100 Hz and shot noise at higher frequencies.

3.2. Optics

The Virgo otpical design imposes very large (diameter 350 mm) and heavy optics (20 kg) for the interferometer suspended mirrors and beam splitter. The total losses at 1064 nm of each mirror (including absorption, scattering and large-scale wavefront deformation) should not exceed 100 parts per million (ppm). There are specific constraints on the absorption (< 5 ppm) due to the thermal lensing and on the scattering level (< 5 ppm) to minimize the noise on the interferometer output, due to the scattered light. For these reasons mirrors and beam splitters are super-polished pieces made of a new types of silica (Suprasil 311 SV, Suprasil 312 SV), with very low absorption and scattering, manufactured by the German company Heraeus, developed in collaboration with ESPCI (Paris). The OH content is very low («50 ppm), the refractive index is homogeneous in all directions and the birefringence is very low (< 5.10-4 rad/cm). The bulk absorption of the silica substrates crossed by the VIRGO laser beam has been measured [13] as being less than 0.7 ppm/cm. The flatness of these large components is 8 nm RMS on 150 mm. The limiting factor of the wavefront flatness is the substrate: since the polishers can not guarantee every time better wavefronts, the substrate surface is corrected before deposition by using a Corrective Coating technique [14]. The mirrors, after final coating with reflective quarter wavelength layers of SiO_2 and Ta_2O_5, exhibit a global RMS flatness of the order of 3 nm over 150 mm, an average absorption of less than 1 ppm

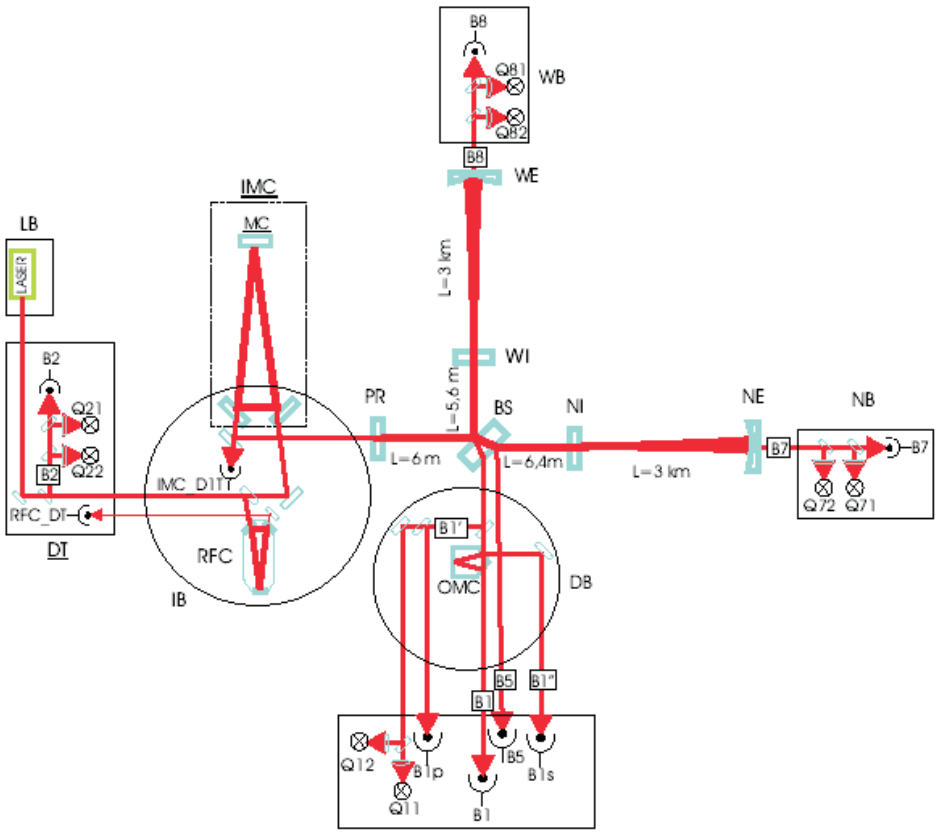

Figure 2. Virgo optical layout

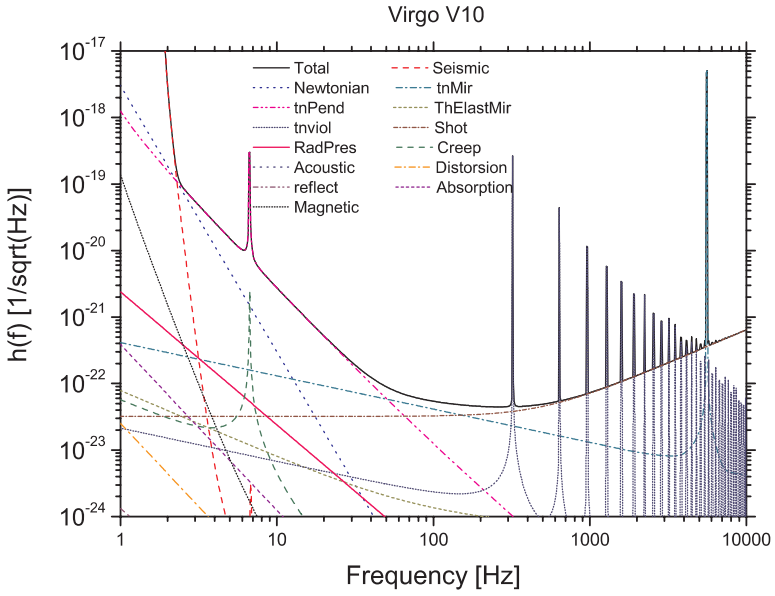

Figure 3. Virgo design sensitivity with the limiting noise sources: seismic noise up to 4 Hz, thermal noise up to 100 Hz and shot noise at higher frequencies.

and a scattering of the order of 5 ppm, thus being the most performing existing large optics.

3.3. Suspensions

In all the present ground based interferometer the test masses are mirrors, isolated from the ground by suspending them to pendula. The Virgo seismic isolation, being more complex than those of the detectors, provides the highest passive isolation performance. The test masses are located in an ultra-high vacuum system (from 10^{-9} mbar for H_2 up to 10^{-14} for hydrocarbon) and suspended from a sophisticated seismic isolation system the Superattenuator (SA). The SA is a multistage, 10-m-tall, multipendular suspension, which is effective in isolating the test masses from the seismic noise for frequency higher than a few Hz (the pendulum resonance frequency are all confined below a couple of Hz). The seismic attenuation system is either passive and active. The passive filtering is provided by the SA, a chain of mechanical filters. The first stage of the SA [15] is an inverted pendulum (IP) preisolating stage [16]. A chain of five mechanical filters is suspended from the top of the IP. From the last stage of the chain (the so called "filter 7" [17]) an anvil shaped steel stage, the so called "marionette" [18], is suspended by a steel wire. The payload, suspended from the marionette, is formed by the test mass and by an aluminum reference mass (RM), independently suspended behind the mirror. The passive attenuation of the whole chain is better than 10^{-14} at 10 Hz, corresponding to an expected residual mirror motion of $10^{-18}\mathrm{m}/\sqrt{\mathrm{Hz}}$ at the same frequency. Due to the residual low frequency motion of tens of microns at the resonances of the SA, the frequencies of the whole chain normal modes ranging between 40 mHz and 2 Hz with quality factors up to 10^3, the SA is designed to allow an active control of the mirror position over a very large dynamic range. In order to allow lock acquisition, i.e. to confine the residual mirror motion below 1μm, control forces are exerted on three actuation points: at the IP top stage level, performing an inertial active damping of the resonant motions of the SA [19]; using the marionette coils to steer the suspended mirror [18] with respect to the last stage of the chain; and directly on the mirror, through coils supported by the RM which can act on four magnets mounted on the holder of the mirror. A local control system referred to the ground, is active in the bottom part of each SA in order to keep the longitudinal displacement of the mirrors below 1μm rms. It uses as a signal two laser beams emitted by lasers leaning on ground outside each tower. These beams enter into the tower through an optical window, one is reflected one by a mirror on the marionetta and the other one by the suspended mirror itself, and then impinge on respective PSD detectors, after passing through dedicated optical systems, thus being used as optical levers for reconstructing the mirror movements. A correction feedback using this signals allows to damp and control the local angular motion of the mirrors below 1μrad RMS and makes the acquisition of the longitudinal lock of the interferometer possible with a limited actuation force, thus preventing noise reintroduction in the detection band. Since this system is referred to the ground, and therefore limited by the seismic noise, once the longitudinal locking of the interferometer is acquired the local control system is switched off and replaced by the automatic alignment system.

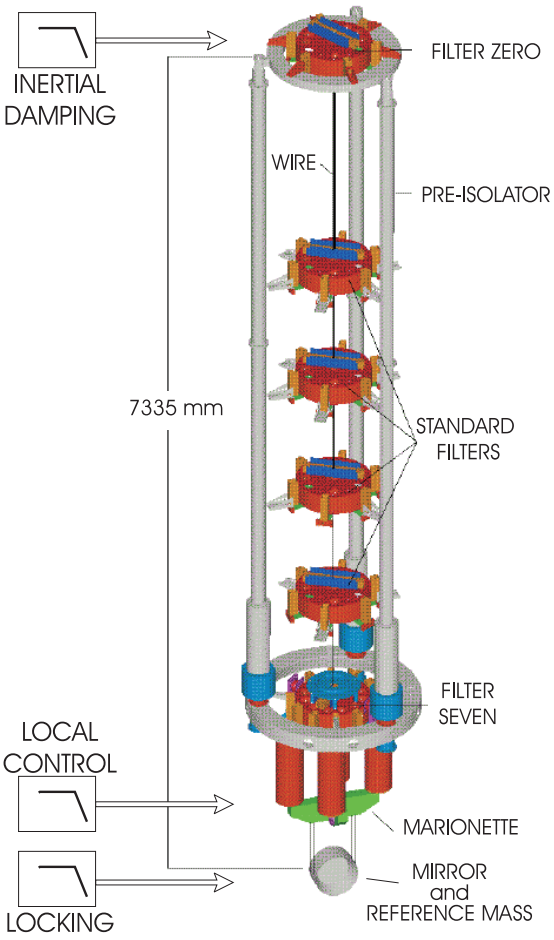

Figure 4. Scheme of the Virgo Superattenuator chain: in the CITF the feedback is exerted at three stages: inertial damping is performed at the inverted pendulum stage, local control through the marionette, and the interferometer locking keeping force acts on the mirror through the reference mass.

4. The commissioning of the 3 km long VIRGO

In order to test the stability and robustness of all of the sub-systems involved in the operations and to get some experience in designing the various control systems, the Virgo commissioning activity has been organized in steps of increasing complexity: the separate commissioning of the North and West Fabry-Perot cavities, followed by the commissioning of the recombined Michelson Fabry-Perot ITF, and eventually the commissioning of the recycled Michelson Fabry-Perot ITF. Short periods of continuous data-taking (the so-called commissioning runs) have taken place every two to three months since November 2003, in order to check the evolution of the detector and the consequent progress in the level of sensitivity. Five commissioning runs have been performed so far:

- C1 - North cavity longitudinally controlled (14-17 November 2003);
- C2 - North cavity longitudinally controlled, plus automatic alignment (20-23 February 2004);

- C3 - Two configurations: North cavity as in C2 plus the frequency stabilisation servo (23-26 April 2004); first data-taking with the ITF locked in recombined mode (26-27 April 2004);
- C4 - ITF longitudinally controlled in recombined mode, with suspension tidal control, automatic alignment on both the arms, frequency stabilization servo (24-29 June 2004);
- C5 - Two configurations: ITF in recombined mode as in C4, plus end suspensions with full hierarchical control (2-6 December 2004); first data-taking with the ITF locked in recycled mode (6-7 December 2004);

The commissioning of a single arm was concluded with C3, with an automatic alignment and a frequency servo running for this configuration. The evolution of the detectors working in recombined and in recycled mode will be described in sections 4.2 and 4.5, where the attention will focus upon the two most recent data-taking during C4 and C5.

4.1. The longitudinal control

The nominal sensitivity of an interferometric detector such as Virgo is achieved by selecting an appropriate working point, with laser light resonant in the optical cavities, and the output port tuned on the dark fringe. These conditions translate into fixed relationships between the laser light wavelength and four independent lengths of the ITF [20]:

- the length of the recycling cavity (PRCL),
- the differential length of the short Michelson arms (MICH), $l_1 - l_2$;
- the common (CARM) and the differential (DARM) length of the two long arms, $L_1 + L_2$ and $L_1 - L_2$.

While the expected sensitivity is of the order of 10^{-18} m/$\sqrt{\text{Hz}}$, the allowed deviation from the working point is 10^{-12} m rms. A feedback control system is needed to keep the ITF locked on the required interference conditions. Relative displacement of the mirrors is detected using a carrier beam phase modulated at 6 MHz. Using a standard PDH technique all the lengths involved can be reconstructed by mixing the signals produced by the photodiodes, which are placed at different output ports of the ITF. These error signals are digitized and sent to the Virgo global control system (Global Control [20]), which computes the corrections to be applied to the mirrors by the actuators at the level of the reference mass.
A local control system, referred to the ground, is active in the bottom part of each SA in order to keep the longitudinal displacement of the mirrors below 1μm rms. This also keeps the local angular motion of the mirrors below 1μrad rms and allows the acquisition of the longitudinal lock of the interferometer using a limited actuation force, thus preventing noise reintroduction in the detection band.

4.2. The recombined interferometer

As an intermediate step towards the full configuration, the interferometer was commissioned in recombined mode for a large part of 2004. In this mode the optical scheme differs from

the final configuration in that the PR mirror is significantly misaligned, so that only three lengths instead of four have to be longitudinally controlled: CARM, DARM and MICH. Using the end transmitted signals the two long arms can be controlled independently, acting on the corresponding end mirrors. As soon as the cavities are locked, MICH is controlled with the output port demodulated signal (or alternatively the reflected demodulated signal) filtered and sent to the BS. By applying this strategy the lock is usually acquired in a few seconds.
Because of the low power upon the end photodiodes, the transmitted signals are electronic noise-limited: once the lock is acquired, they have to be replaced by another set of less noisy signals. In a steady state CARM is also attained using by the in-phase demodulated component of the light reflected by the ITF. Instead, DARM is attained by the in-phase output port light, which is slightly contaminated by MICH, mainly provided by the other quadrature of the ITF reflected light. Linear combinations of the error signals are computed to provide the correction forces to the mirrors. This phase is called linear locking.

4.3. The Commissioning Run C4

During C4, the interferometer was operated for five days in recombined mode. The longitudinal degrees of freedom were locked according to the linear locking scheme previously described, with the automatic alignment running on both arms and suspension tidal control on the end mirrors. The laser frequency was actively stabilized on CARM, which was locked on the reference cavity in line with the frequency servo strategy developed in Virgo, the so-called Second Stage of Frequency stabilization. The OMC was locked on the dark fringe, so that DARM could be controlled by the filtered output demodulated signal. The interferometric scheme in the data-taking mode is described in figure 5. The longest continuous lock during C4 was about 28 hours. All 9 lock losses that occurred were analyzed and understood. At the beginning of the run some acoustic noise injection was performed in the laser and detection laboratory, to study the possible couplings with the dark fringe signal [21]. A software and hardware injection of inspiral events was also performed [23] during the data-taking, to test some of the elements of the analysis chain and to characterize the detector stability during the run.
At the beginning of the run some calibration noise injection was performed in order to produce the sensitivity curve. The result is plotted in figure 6, together with the main noise contributions. The sensitivity is still limited by control noise at low frequency, by the mirror actuator noise in the intermediate frequency range and by laser frequency noise, starting from some hundreds of Hz.

4.4. Reduction of actuation noise

Longitudinal control during C4 was acquired and maintained by acting on the mirror at the level of the reference mass. The noise injected by the recoil mass actuators into the interferometer is a severe limit to the sensitivity of Virgo: at 20 Hz it is more than 1000 times larger than the design sensitivity. It is mainly contributed to by the 16 bit DAC noise (300 nV/sqrt(Hz)) and the coil driver noise (70 nV/sqrt(Hz)) and is converted into equivalent mirror

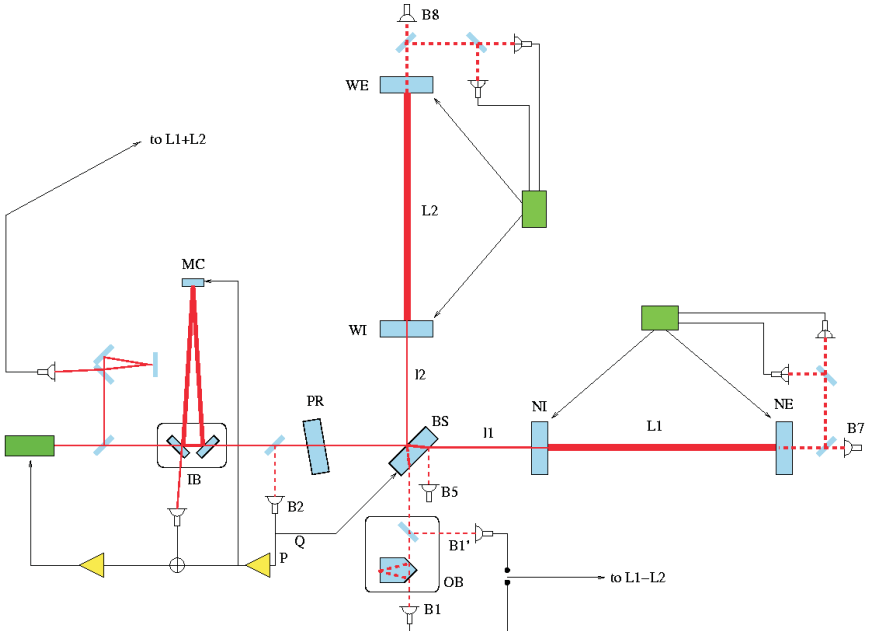

Figure 5.C4 configuration: the data-taking mode consisted of the ITF locked in recombined mode according to the linear locking scheme, with the automatic alignment running on both arms. In this state, the frequency stabilization control system is engaged. With the laser frequency pre-stabilized on the IMC, the CARM locking loop is switched off and the corresponding PDH error signal is added into the error point of the IMC-loop (bandwidth 1 kHz). The same signal is applied to the length of the IMC, with a bandwidth of about 200 Hz: in this way the laser frequency and the length of the IMC are stabilized on CARM, which provides a better frequency stability at frequencies higher than the internal resonances of the SA. The low frequency stabilization is achieved locking CARM on the RFC length.

displacement by a reasonably large coupling factor: 130 microns/V. Such a large coupling factor has been adopted in order to ease the lock acquisition. Once the lock is acquired, the residual force to be exerted is largely in the low frequency region (DC-5 Hz), where tidal drifts and resonant motion have to be compensated, and very small elsewhere. Therefore, the gain of the coil driver (and the corresponding noise) cannot be reduced, unless a large fraction of the low frequency force is reallocated to the upper stages. This is in fact the Virgo suspension hierarchical control strategy: once the lock is acquired, the locking force is split over three actuation stages in a hierarchical way. The correction in the range DC-0.01 Hz, that compensates for earth tides, is reallocated upon the soft inverted pendulum; the force in the range 0.01-8 Hz, where all the suspension resonances fall, is reallocated to the marionette. Consequently, the residual force on the reference mass is strongly reduced, and a strong reduction of the coil driver gain becomes possible.

With respect to the reference mass-mirror system, the upper actuation stage reveals more complex dynamics. There is an intrinsic and non negligible coupling between the horizontal actuators pushing on the marionette and the pitch motion induced on the mirror. Therefore, the locking of the ITF from the marionette, requires the use of all four actuators available with a proper frequency dependent diagonalization.

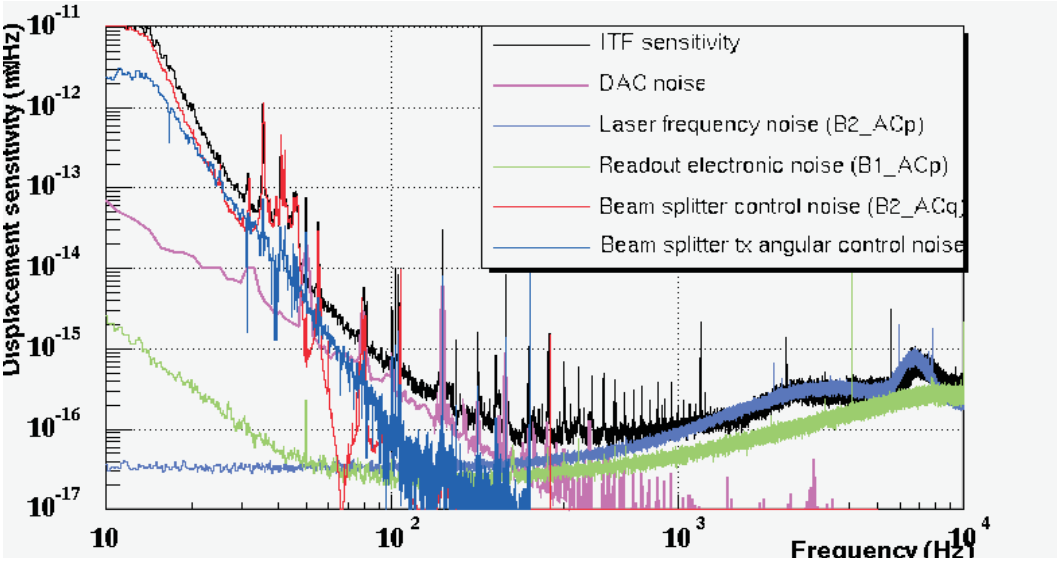

Figure 6. Sensitivity curve in C4 expressed in $m/\sqrt{Hz}$, with the main noise contributions: control noise at low frequency, mirror actuator noise (essentially 16 bit DAC noise) in the intermediate frequency range and laser frequency noise starting from some hundreds of Hz.

Once the lock is acquired using the recoil mass only, the recombined ITF should be fully locked before reallocating the force to the upper stage: it is necessary that second stage of frequency stabilization is engaged, otherwise the frequency noise would cause saturation of the marionette actuators. After reallocation, the reference mass residual correction always remains below 10 mV, allowing a reduction of the coil driver amplification by a factor of 1000.
The ITF was running in recombined mode during the first part of C5, when a full hierarchical control of the end suspensions was successfully tested.

4.5. The lock acquisition of the recycled ITF

As Virgo and LIGO have similar optical set-ups, the lock acquisition strategy developed [24] and adopted in the LIGO interferometer [25] was taken as a starting point for the lock acquisition scheme of the Virgo recycled interferometer. This baseline technique consists in sequentially controlling the four degrees of freedom of the ITF, dynamically changing the optical sensing matrix to compensate the variation of the fields in the course of lock acquisition. Some intermediate stable states were locked applying the LIGO strategy, and some full lock acquisition trials were performed. At the same time an alternative technique was developed: the first tests rapidly provided promising results, and experimental activity on the baseline technique was subsequently interrupted.

4.6. Lock acquisition

The basic idea of the new lock acquisition technique is that the ITF is locked outside the working point for the dark fringe. In this way a good fraction of light escapes through the output port and the power build-up in the recycling cavity is low. Then the ITF is adiabatically brought on to the dark fringe. This technique is referred to as variable finesse [22], because the finesse of the recycling cavity changes during the lock acquisition path. The procedure starts with the PR mirror initially misaligned by some μrads. The simple Michelson is controlled on the half fringe, using the output port DC signal, while the two arms are independently locked using the end photodiodes, as in the recombined configuration. The power recycling cavity length is controlled using the reflected 3f-demodulated signal. In this way all the four longitudinal degrees of freedom of the ITF are locked in a stable way from the beginning of the lock acquisition procedure, preventing excitation of the mirrors. From this starting condition the PR is realigned, while always maintaining the Michelson on the half fringe, giving a very low recycling gain.
In order to increase the recycling gain the Michelson has to be brought on to the dark fringe: this is done adiabatically, decreasing the offset in the Michelson error signal. At the same time, the control scheme changes. The end photodiodes can only be used to independently control the cavities when the ITF is far from the dark fringe: when nearing the dark fringe they begin to couple strongly and a common and differential control has to be activated to keep the lock. Then a frequency stabilization servo is engaged, controlling CARM with a very high bandwidth: consequently, the contamination by this degree of freedom on all the photodiodes is cancelled. DARM is kept in a locked state by one of the end photodiode signals. The final step consists of switching from the DC to a demodulated signal to control the Michelson length. Eventually the offset in the Michelson error signal is removed, the ITF goes on to the dark fringe and the recycling cavity gain increases up to the maximum value.
Applying this technique the lock acquisition of the full Virgo ITF was reached for the first time on 26th October 2004, and tested in the latter part of C5. A typical lock acquisition sequence takes few minutes and it provides a deterministic and repeatable lock. The final recycling cavity gain was measured to be around 25.

4.7. Sensitivity progress

The 3 km Virgo detector has been in commissioning for about one and half years. The first lock of a single Fabry-Perot arm was realized in October 2003: after exactly one year, the lock of the recycled ITF was performed (see figure 7). In between, the commissioning of the recombined ITF was also realized, with the continous improvement of the various sub-systems and controls involved in the operations: longitudinal lock, automatic alignment, frequency stabilization servo, full hierarchical suspension control.
During this one-year period the displacement sensitivity of the detector has evolved from $10^{-11}\mathrm{m}/\sqrt{\mathrm{Hz}}$ to less than $10^{-16}\mathrm{m}/\sqrt{\mathrm{Hz}}$.

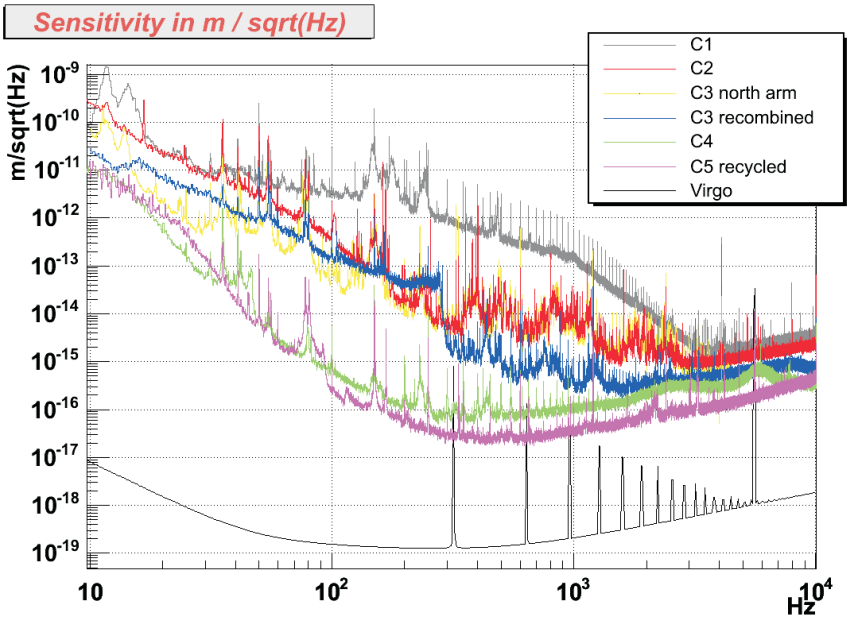

Figure 7. Progress in the Virgo sensitivity in approximately one year of commissioning. The fact that during the summer of 2004 a laser power attenuator was installed in the injection system also need to be considered: in C5 the laser light entering the ITF was around 0.7 W, instead of 7 W as in the previous runs.

5. Conclusion

The gravitational wave interferometers are the extreme evolution of the classical Michelson interferometer. Even if their goal is the measurement, at the typical frequency of 100 Hz, of spectral densities of relative displacements, rather than static lengths, the order of magnitude of the target sensitivity (much less than the diameter of an atomic nucleus) sounds astounding. The progress in the sensitivity of the Virgo interferometer towards the target sensitivity is a good demonstration of the way in which this measurements can be attained. After one year of upgrades, the displacement sensitivity of the detector has evolved from $10^{-11}\mathrm{m}/\sqrt{\mathrm{Hz}}$ to less than $10^{-16}\mathrm{m}/\sqrt{\mathrm{Hz}}$. Presently, the commissioning of the recycled ITF is on-going, with the goal to improve the robustness of the longitudinal lock, at the same time putting into operation other main control system successfully implemented in the recombined configuration and reducing external noise sources. The characterization of the noise contributions to the sensitivity constitutes another fundamental task, with the prospect of a science run, close to the target sensititivy, before the end of 2005.

References

[1] A A Michelson and E W Morley, Philos Mag S 5, 24 (151), 449-463 (1887).
[2] F. Acernese et al., Status of Virgo, Class Quant Grav., 21, 385–393 (2004).

[3] D. Sigg et al., Commissioning of the LIGO detectors, Class Quant. Grav., 19(7), 1429–1435 (2002).
[4] M Ando et al., Current status of TAMA, Class Quant. Grav. 19(7), 1409–1419, (2002).
[5] B. Willke et al., The GEO 600 gravitational wave detector, Class Quant. Grav., 19(7), 1377–1387 (2002).
[6] M E. Gertsenshtein, V I. Pustovoit, Soviet Physics, JETP, 16, 433, (1962).
[7] R V. Pound, Electronic Frequency Stabilization of Microwave Oscillators, Rev. Sci. Instrum. 17 490-505 (1946)
[8] R W P. Drever et al., Laser phase and frequency stabilization using an optical resonator, Appl. Phys. B: Photophys. Laser Chem. 31 (1983) 97-105
[9] L. Schnupp, The European Collaboration Meeting on Interferometric Detection of Gravitational Waves, 37, 66, 92, (Sorrento, 1998).
[10] Morrison E., Meers B J., Robertson D I., Ward H., Automatic alignment of optical interferometers, Appl Opt., 33, 5041 (1994).
[11] D. Z. Anderson, Alignment of resonant optical cavities, Appl. Opt. 23 2944-2949 (1984).
[12] D. Babusci, H. Fang, G. Giordano, G. Matone, L. Matone, V. Sannibale, Alignment procedure for the VIRGO interferometer: experimental results from the Frascati prototype, Phys. Lett A 226, 31-40 (1997).
[13] L. Pinard et al., Optical Systems design 2003 proc., 2003.
[14] JM Mackowski et al., Opt Quant Electr., 31(5/7), 507–514, (1999).
[15] G Ballardin et al., Measurement of the VIRGO superattenuator performance for seismic noise suppression, Rev. Sci. Instrum. 72 3643-3652 (2001).
[16] G Losurdo et al., An inverted pendulum pre-isolator stage for the VIRGO suspension system, Rev. Sci. Instrum., 70(5), 2507-2515 (1999).
[17] G. Ballardin et al., Measurement of the transfer function of the steering filter of the VIRGO superattenuator suspension, Rev. Sci. Instrum., 72, 3635 (2001).
[18] M. Bernardini et al., Suspension last stage for the mirrors of the VIRGO interferometric gravitational wave antenna, Rev. Sci. Instrum., 70, 3463 (1999).
[19] G. Losurdo et al., Inertial control of the mirror suspensions of the VIRGO interferometer for gravitational wave detection, Rev. Sci. Instrum., 72, 3654-3661 (2001).
[20] F. Cavalier, Le controle global de Virgo, These d'Habilitation a diriger des Recherches, Université de Paris Sud, LAL 01-69 (2001).
[21] I. Fiori, A first study of environmental noise coupling to the Virgo interferometer, these proceedings.
[22] L. Barsotti et al, Status of Virgo, Class. and Quant. Grav., proc. GW DAW 2004., to be published.
[23] L B. Bosi, Inspiral analysis of the Virgo commissioning run 4, these proceedings.
[24] M Evans, Lock acquisition in Resonant Optical Interferometers, PhD Thesis, CALTECH (2001)
[25] M Evans et al., Lock acquisition of a gravitational-wave interferometer, OPTICS LETTERS vol.27, n.8. April 15, (2002)
[26] K Arai and the TAMA collaboration Sensing and controls for power-recycling of TAMA300, submitted to Class. Quantum Grav.